in prion diseases. Because the serum-free supernatant of *Prnp*$^{+/+}$ cell cultures could not rescue the phenotypes of *Prnp*$^{-/-}$ cells, PrP^{C} might act autonomously. Our *in vitro* system provides a new way to detect the cellular function of PrP^{C} in nerve cells and to establish the molecular mechanisms of apoptosis involving PrP^{C}.

Chieko Kuwahara*, Alice M. Takeuchi*, Takuya Nishimura*, Keiko Haraguchi*, Atsutaka Kubosaki*, Yasunobu Matsumoto*, Keiichi Saeki*, Yoshitsugu Matsumoto*, Takashi Yokoyama†, Shigeyoshi Itohara‡, Takashi Onodera*

**Department of Molecular Immunology, School of Agricultural and Life Sciences, University of Tokyo, Bunkyo-ku, Tokyo 113-0032, Japan*
e-mail: aonoder@hongo.ecc.u-tokyo.ac.jp
†National Institute of Animal Health, Tsukuba, Ibaraki 305-0852, Japan
‡Laboratory for Behavioural Genetics, Brain Science Institute, RIKEN, Wako, Saitama 351-0198, Japan

1. Bueler, H. *et al. Nature* **356,** 577–582 (1992).
2. Collinge, J. *et al. Nature* **370,** 295–297 (1994).
3. Tobler, I. *et al. Nature* **380,** 639–642 (1996).
4. Sakaguchi, S. *et al. Nature* **380,** 528–531 (1996).
5. Lledo, P. M. *et al. Proc. Natl Acad. Sci. USA* **93,** 2403–2407 (1996).
6. Weissmann, C. *Curr. Biol.* **6,** 1359 (1996).
7. Ryder, E. F., Snyder, E. Y. & Cepko, C. L. *J. Neurobiol.* **21,** 356–375 (1989).
8. Onodera, T., Ikeda, T., Muramatsu, Y. & Shinagawa, M. *Microbiol. Immunol.* **37,** 311–316 (1993).
9. Tsujimoto, Y. in *Apoptosis: Mechanisms and Role in Disease* (ed. Kumar, S.) 137–156 (Springer, Berlin, 1998).
10. Kurschner, C. & Morgan, J. I. *Brain Res. Mol. Brain Res.* **30,** 165–168 (1995).

Breast-cancer diagnosis using hair

James *et al.*[1] observed a difference between the X-ray diffraction patterns of hair from healthy females and from breast-cancer patients. This difference was reported as the presence of an extra ring corresponding to a spacing of 4.44 nm on the patterns obtained from breast-cancer patients. This ring was also observed in patterns from subjects "not yet diagnosed with breast cancer but suspected of being at risk". James *et al.* proposed that these observations might lead to a screening method for breast cancer. We have now repeated the study using a different hair type (from the scalp), but are unable to replicate their observations.

The existence of a ring at a spacing of 4.5 nm was first attributed to 'lipid crystals'[2] that could be removed only by prolonged extraction in hot solvents. Our experience[3,4] and that of our colleagues from l'Oréal[5] confirms the presence of intense diffraction ring(s) arising from lipids in keratinous tissues. We recently performed a microdiffraction analysis on beamline ID13 at the ESRF

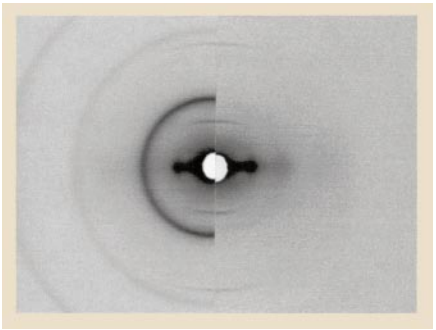

Figure 1 Split X-ray diffraction pattern. Left, scalp hair from healthy subject, displaying intense rings arising from lipid granules; right, hair from breast-cancer patient, with no clear rings.

and observed in human hair and other tissues that the lipid granules are mainly located in the outer part of the tissue[6]. We are therefore unable to explain the lack of the ring at 4.5 nm in the diffraction pattern of normal hair reported by James *et al.* One possibility is that working with a microbeam inhibited the observation of the ring because the lipid granules took up unfavourable orientations.

To compare X-ray diffraction patterns of hair from healthy subjects and breast-cancer patients under the same experimental conditions, we conducted experiments at station D43 of the synchrotron source LURE (Université Paris-Sud). We compared diffraction patterns of scalp hair from ten supposedly healthy people (seven females and three males) with the patterns from ten breast-cancer patients (all female). We irradiated a bundle of hair in a glass capillary with a 0.5-mm monochromatic X-ray beam. The diffraction patterns from healthy subjects displayed an intense ring at 4.48 ± 0.05 nm. The variability of the patterns from breast-cancer patients was larger, but the ring was intense for one patient, of low intensity for seven others, and not observable for the remaining two.

Our observations differ from those of James *et al.* in two main respects. First, we observed the diffraction ring at 4.5 nm on patterns from all healthy subjects (100%, against 22% by James *et al.*). Second, the ring is present in eight out of ten patterns from breast-cancer patients (instead of the 100% observed by James *et al.*). This conclusion is illustrated in Fig. 1: in two out of ten cases, our split patterns between healthy and breast-cancer subjects are exactly the opposite of that of James *et al.* However, it should be remembered that the studies used different hair types.

Fatma Briki*, Bertrand Busson*, Bruno Salicru†, François Estève‡, Jean Doucet*

**LURE, Bât 209-D, Université Paris-Sud, B.P. 34, 91898 Orsay Cedex, France*
†Clinique du Mail, 43-45 Avenue Marie Reynoard, 38100 Grenoble, France
‡Unité IRM, CHU Grenoble, JERSRM, Université Joseph Fourier, B.P. 27, 38043 Grenoble, France

1. James, V., Kearsley, J., Irving, T., Amemiya, Y. & Cookson, D. *Nature* **398,** 33–34 (1999).
2. Fraser, R. D. B., MacRae, T. P., Rogers, G. E. & Fushie, B. K. *J. Mol. Biol.* **7,** 90–91 (1963).
3. Briki, F., Busson, B. & Doucet, J. *Biochim. Biophys. Acta* **1429,** 57–68 (1998).
4. Busson, B., Briki, F. & Doucet, J. *J. Struct. Biol.* **125,** 1–10 (1999).
5. Franbourg, A., Leroy, F., Lévêque, J. L. & Doucet, J. 5th Int. Conf. Biophysics and Synchrotron Radiation, Grenoble (ESRF, Grenoble, 1995).
6. Busson, B., Engström, P. & Doucet, J. *J. Synchotron Rad.* (in the press).

Editorial note Full experimental details of the work by James *et al.* have been published[1,2]. Detailed set-ups for the three different beamlines and links are available from http://www.ansto.gov.au/natfac/asrp.html

1. Wilk, K. E., James, V. J. & Amemiya, Y. *Biochim. Biophys. Acta* **1245,** 392–396 (1995).
2. James, V. J., Wilk, K. E., McConnell, J. F. & Baranov, E. P. *Int. J. Biol. Macromol.* **17,** 99–104 (1995).

Evolution of cooperation between individuals

Nowak and Sigmund[1] conclude that cooperation may have evolved through indirect reciprocity by image scoring. Their simulations[1] and analytical models[1,2] predict long-term cyclical dynamics between cooperative and defector populations rather than an evolutionarily stable equilibrium. Here we add a realistic feature to their model: that there are always some individuals unable to cooperate owing to their poor phenotypic condition (we call these individuals 'phenotypic defectors'). The presence of phenotypic defectors paradoxically allows persistent discriminating cooperation under a much wider range of conditions than found by Nowak and Sigmund because there is selection against both defection and unconditional altruism. In real populations there will nearly always be some level of defection because phenotypic defectors (such as the young, sick or handicapped) may be unable to help even if they have a genetic predisposition to do so.

To test the effect of phenotypic defection, we analysed Nowak and Sigmund's model[1] of indirect reciprocity. In their scheme, each individual has a genetic strategy (k) and a non-heritable image score (s). The image of an individual is crucial in determining whether or not it will receive help from others. The image score is zero at birth, increases by one with every cooperative interaction, and decreases by one with every defection (decision not to donate). In each generation, interactions between pairs of individuals occur at random, with donors cooperating only if the recipient's image score is greater than or equal to the donor's genetic strategy, k ($s \geq k$). The strategies of individuals are permitted to lie between $k = -5$ (unconditional cooperation) and

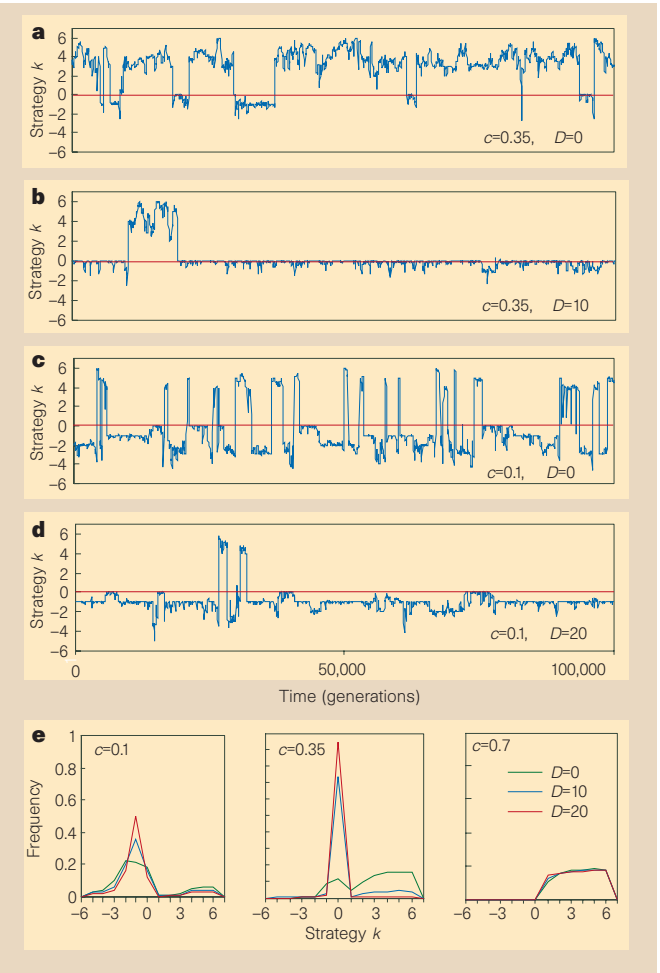

Figure 1 Computer simulations of the model[1] with N=100 individuals, D phenotypic defectors and different costs of cooperation c. **a–d,** Average strategy $\langle k \rangle$ of the population over a simulation of 100,000 generations for different c and D. **e,** Frequency distribution of strategies sampled over 10^7 generations with low, intermediate and high costs of cooperation, and with various numbers of phenotypic defectors, D. Model parameters are as in ref. 1, with $b=1$, mutation rate $p=0.001$, and $m=300$ random interactions per generation. As in ref. 1, after every generation the number of offspring of each player is determined by the fitness accumulated over a lifetime of interactions, and the population strategies evolve by selection and mutation over many generations.

$k=+6$ (pure defection), with $k=0$ indicating a 'discriminating' strategy. The cost to the donor's fitness for each cooperation is c and the recipient's benefit is b.

We modified this scheme and allowed a population of $N=100$ individuals to carry D phenotypic defectors. We assigned the non-heritable phenotypic strategy $k=+7$ to D randomly chosen individuals every generation, but we left unchanged the heritable genotypic strategies of these defectors.

We first consider the effects of phenotypic defectors in a model in which the costs of cooperation are intermediate compared with the benefit of the beneficiary ($c=0.35$, $b=1$). In the absence of phenotypic defectors ($D=0$), the simulation model[1], which incorporates mutation and drift, generally results in a population consisting almost entirely of defectors (Fig. 1a). However, upon the introduction of $D=10$ phenotypic defectors, the population structure becomes dominated by discriminating altruists whose average strategy is mostly $\langle k \rangle = 0$ (Fig. 1b). Over 10^7 generations, the introduction of phenotypic defectors increases the overall frequency of discriminators ($\langle k \rangle = 0$) from 12% ($D=0$) to 74% ($D=10$) and even 95% ($D=20$) (Fig. 1e, middle). These results demonstrate that phenotypic defectors, who are unable to provide help, may nevertheless be central to the evolution of cooperation.

We turn now to the model in which the cost of cooperation is relatively low[1] ($c=0.1$). With no phenotypic defectors ($D=0$), the simulation model yields long-term cycling in the average strategy index, generally with cooperative populations ($\langle k \rangle \leq 0$), but with defectors invading occasionally (Fig. 1c). Although the population initially consisted mostly of cooperators, the introduction of 20 phenotypic defectors led to discriminating cooperators being favoured (at $\langle k \rangle = -1$), effectively suppressing this cycling dynamic (Fig. 1d).

The paradoxical effect whereby phenotypic defectors stabilize discriminate altruism can be explained analytically (see http://lynx.tau.ac.il/coop.html). Whenever there are defectors in the population, there is a persistent advantage for discriminators over non-discriminating altruists because discriminators avoid paying the costs of helping defectors. This advantage disappears as soon as all defectors are eliminated from the population, as often occurs in the Nowak and Sigmund model[1]. In our model, however, a constant supply of phenotypic defectors ensures that the advantage persists, leading to a large population of discriminators that deny help to real genotypic defectors and hence block their invasion.

Our study also shows that the qualitative effect of phenotypic defectors is highly dependent on the cost of cooperation, c (Fig. 1e). A high cost ($c=0.7$) leads to a population of defectors ($\langle k \rangle > 0$) no matter how many phenotypic defectors D are added. However, for intermediate costs ($c=0.35$), the addition of only a few phenotypic defectors strongly increases discriminate altruism (Fig. 1b, e). For low costs ($c=0.1$), where the population is initially cooperative with long-term cycling (when $D=0$), the addition of phenotypic defectors tends to suppress the cycling dynamic.

In the Nowak and Sigmund model[1], the relative frequencies of discriminators and non-discriminators fluctuate during the long-term population cycling, whereas our model predicts that, in cooperative societies, non-discriminators will be replaced by discriminators when the cost of cooperation increases. This implies the evolution of a society in which cheap donations are given unconditionally to everyone, whereas more costly gifts are given discriminatingly, and only to those individuals who can afford to donate such gifts to others (those who are in good phenotypic condition). Evidence for costly help being provided unconditionally to poor phenotypes may not be explained by indirect reciprocity, but rather by alternative theories[3–5].

Arnon Lotem, Michael A. Fishman, Lewi Stone

Department of Zoology, Faculty of Life Sciences, Tel-Aviv University, Tel-Aviv 69978, Israel
e-mail: lotem@post.tau.ac.il

1. Nowak, M. A. & Sigmund, K. *Nature* **393,** 573–577 (1998).
2. Nowak, M. A. & Sigmund, K. *J. Theor. Biol.* **194,** 561–574 (1998).
3. Hamilton, W. D. *J. Theor. Biol.* **7,** 1–52 (1964).
4. Zahavi, A. in *Evolutionary Ecology* (ed. Stonehouse, B. & Perrins, C. M.) 253–259 (Macmillan, London, 1977).
5. Roberts, G. *Proc. R. Soc. Lond. B* **265,** 427–431 (1998).

Higher fullerenes in the Allende meteorite

Fullerenes (C_{60} and C_{70}) were discovered during investigations of the mechanism by which carbon molecules form in interstellar and circumstellar shells[1]. Unlike diamond and graphite, the other pure forms of carbon, fullerenes are extractable in an organic solvent such as toluene, which led to the detection of the higher fullerenes (C_{100} to C_{250}) in carbon-arc-evaporated soot material[2]. We have applied a similar solvent extraction procedure to an acid residue of the carbonaceous chondrite from the Allende meteorite to search for higher fullerenes. We found C_{60} and C_{70}, as well as a unique distribution of remarkably stable clusters of C_{100} to C_{400}. These large extraterrestrial carbon clusters are either the first indication of higher fullerenes or are an